JOURNAL OF
EMERGING INVESTIGATORS

Article

Investigating intertidal sediment sorting and median particle diameter variation on an eroding beach face

Damien Crowley[1], Christopher Kozak[1]
[1] Wantagh High School, Wantagh, New York

SUMMARY

Climate change and rising sea levels are worsening coastal erosion, endangering coastal economies, communities, and ecosystems. Beach nourishment projects seek to combat this erosion, but the lack of information about spatial grain size variation and sediment transport systems limits the success of current efforts. It is imperative to understand these properties to accurately predict the retention of nourishment sediment after beach nourishment occurs. In this study, we investigated how grain size varies spatially on two example fields at Jones Beach, New York, to provide further insight into how sediment is sorted in the transport direction on beach faces. We chose Fields 4 and 5, public beach sites at Jones Beach on the southern coast of Long Island, as the study site because of their popularity and extensive developmental status, meaning coastal erosion could hinder future recreation and construction. Based on previous sediment transport models, we hypothesized that the sediment along the coastline of Fields 4 and 5 becomes progressively finer and better sorted from east to west. The sieve analysis indicated that median grain size, on average, increased from east to west while sorting remained constant. Offshore wave climate data, consisting of waves' heights and directions, revealed that the site experiences more east-approaching than west-approaching significant wave action. Our findings may enhance sediment transport modeling at Jones Beach and other eroding coastlines, informing beach nourishment projects vital for mitigating erosion.

INTRODUCTION

Coastal erosion, the process by which wave action and ocean currents carry rocks, soils, and sands along the coast, threatens coastal development (1). Sea level rise hastens shoreline erosion, exacerbates coastal flooding, and raises water tables, adversely affecting coastal structures and endangering coastal communities and ecosystems (2, 3). Human activities contributing to rising sea levels have exacerbated the issue. Furthermore, anthropogenic activities, especially greenhouse gas emissions, have raised global temperatures by 1.25°C above the preindustrial average, causing global sea level rise of 21-24 centimeters since 1900 (4, 5). Coastal erosion also hinders the United States' coastal economies by causing nationwide property damage and land destruction valued at nearly $500 million annually (1). Therefore, it is evident that, beyond adversely impacting local ecosystems, coastal erosion can have catastrophic effects in highly developed coastal areas, threatening coastal populations. Despite recent climate reform policies, sea level rise continues to accelerate coastal erosion, underscoring the urgent need for coastal protection from erosion (6).

Beach nourishment—the addition of nonnative sand to a beach to serve as a buffer against coastal erosion—has become a common method for countering shoreline retreat (1). Beach nourishment involves dredging sediment from an alternate source and adding it to an eroding shoreline to elevate or extend it seaward (7). From the first beach nourishment project in 1922 through 2023, 3567 nourishment projects used 1,277,554,795 m^3 of sediment to nourish 1555 km of the US coastline, costing federal agencies, such as the U.S. Army Corps of Engineers, about $8.7 billion (8). Alternative approaches have attempted to prevent coastal erosion by obstructing wave action with wooden and concrete structures (1). However, these non-nature-based shoreline hardening techniques have consistently been found to hinder marsh and coastline migration, while also exacerbating erosion in adjacent coastal regions (1). Therefore, researchers and federal agencies primarily favor soft and nature-based methods (e.g. beach nourishment) because they can absorb and dissipate waves, which reduces coastal erosion without directly preventing wave action itself (1). Despite the benefits of beach nourishment, it is important to note that nourishment projects present unique and intrinsic issues, such as the uncertain longevity of nourishment sediment after a project's completion (1).

Understanding a site's grain size distribution (GSD) —the weight-based percentage of a site's sediment in different size fractions—is crucial for ensuring that post-nourishment sediment matches native GSD and disruption of local ecosystems is avoided (9, 10). Sediment used during nourishment projects is naturally redistributed after placement. To address this redistribution, the overfill factor method is commonly used to predict the volume of borrowed grain that must be applied to the nourishment site to achieve the desired nourishment result (11). The overfill factor method utilizes the GSD of the native and borrowed sediment to predict this necessary volume (11). Therefore, determining these GSDs is essential for ensuring that the nourishment grain in certain size ranges (i.e., 63–100 μm) is not entirely swept away from the nourishment site immediately after placement, and the desired volume remains on site after redistribution. Predicting the necessary volume of nourishment grain can also reduce the possibility of placing an excessive volume of borrowed sediment at the nourishment site, which could burden the

https://doi.org/10.59720/24-146

ecological community even after redistribution occurs (11).

Determining the median particle diameter (D_{50}), or the particle size at which 50% of the sample is finer and 50% is coarser, can improve cross-site modeling by signifying typical on-site grain size (12, 13). Additionally, calculating the uniformity coefficient (CU = D_{60}/D_{10}) of a site's grain can provide insight into how well-sorted the site's grain is (12, 14). For these reasons, GSD studies frequently calculate these values along their sites' longshores (parallel to the seashore) and cross-shores (perpendicular to the seashore) to improve spatial GSD or sediment transport modeling (12). Examining the on-site factors that influence GSD can also help researchers improve their understanding of particle size variation results (12). These factors include the local averages in significant wave heights as well as wave directions, energies, and periods, all of which constitute the wave climate (15). Understanding local wave climate values can aid developers in predicting on-site sediment transport trends, enhancing their ability to select a suitable GSD for beach nourishment material based on a prediction of how grain will redistribute over time (12). Therefore, our study will gather and interpret these statistical values at the study site to enhance our analysis of on-site sediment redistribution and longshore drift.

Generalizing sediment transport models across different coastlines could help hasten erosion control projects by expediting the initial step of analyzing the shore's erosion patterns. However, proposed models are debated in the literature because sediment transport varies greatly between sites due to numerous differentiators, such as topography, particle size, and local wave climate. For instance, the popular McLaren model states that sediment in transport tends to become better sorted and progressively finer while demonstrating increasingly negative skewness—the proportion of finer grains increases compared to coarser ones—in the transport direction compared to the sediment in the direction of its origin (16). However, while testing the accuracy of the McLaren model at the Rhone Delta's coastline, researchers found that D50 and CU progressively decreased in the direction of sediment transport, limiting the application of the McLaren model in determining the longshore transport of sediment in the nearshore zone of a beach face (17). Other researchers studying coasts with multiple sediment sources and directions of sediment transport have also highlighted discrepancies between their analyses of on-site grain size, sorting, and directional transport trends and the predictions of the McLaren model (18–20). As a result, some researchers have proposed that the McLaren model is more applicable when evaluating sediment transport trends at sites with a single sediment input compared to when analyzing sites with multiple sediment sources and transport directions (18-21). Differing from these conclusions, other researchers' sediment transport findings at a tropical microtidal beach agreed with the McLaren model, demonstrating that the McLaren model can be applied effectively in some scenarios (22). The incongruence of past sediment transport findings underscores the difficulty of developing a model for grain erosion that applies consistently across all scenarios, reflecting the complexity of the many variables involved. However, examining the effects of these variables and variations in sediment trends across diverse coastal regions could help refine sediment transport models and improve the efficiency of predicting transport trends at prospective erosion control sites.

We aimed to examine the spatial variation of grain size in the Jones Beach intertidal zone. Previous work has noted that ocean currents flow obliquely from east to west along Jones Beach, New York (an eroding coastline adjacent to the Atlantic Ocean), inducing longshore drift (23, 24). Fields 4 and 5 of Jones Beach were chosen to configure the study site because of their popularity and high developmental status, as coastal erosion could potentially hinder social endeavors and infrastructure in the future (**Figure 1**) (24, 25). Based on the McLaren model and predicted longshore drift at Jones Beach, we hypothesized that the sediment along the coastline of Fields 4 and 5 becomes progressively finer and better sorted from east to west. The GSD results reveal a diagonal-like trend (i.e., coarse outlying sites surrounded by finer sites were found gradually more west and north of the southeast border) at Fields 4 and 5. We found through wave climate analysis that there were more eastward (approaching from the east) significant waves than westward ones south of Fields 4 and 5, supporting the work and findings of the New York State Office of Parks, Recreation, and Historic Preservation (24). Our results also suggested that median grain size increases in the direction of sediment transport along the coastline of Fields 4 and 5 while sorting is constant, contradicting the hypothesis regarding both grain size and sorting variation in the direction of sediment transport. Based on the findings, we proposed a model predicting how sediment transport occurs at the study site. These findings and the proposed sediment transport model are essential for potential future nourishment projects at Jones Beach and may be beneficial for sediment transport modeling on other eroding beach coastlines, facilitating critical beach nourishment projects. Additionally, our findings and their contradiction of the hypothesis limit the application of proposed generalizable sediment transport models in the literature and accentuate the importance of additional intertidal spatial grain modeling studies that accurately adopt generalizable sediment transport models.

RESULTS

We recorded grain size data and directional wave data from 50-gram sediment samples collected along evenly spaced cross-shore transects at Fields 4 and 5, Jones Beach. After collecting samples, we fractionated each sample by diameter using manual sieve analysis, which we averaged and compared to the site's mean distribution. In addition, we calculated the D_{50} of each site from the sieve analysis results, which displayed increased D_{50} spikes at the same sites as shown by the passing percentage plots (**Figure 2**). Through sieve analysis, we showed that the site's low-tide zone's D_{50} = 361 μm, middle-tide zone's D_{50} = 318 μm, and high-tide zone's D_{50} = 389 μm (**Figure 3**).

Additionally, we used the sieve analysis results to calculate each sample's uniformity coefficient (CU) (**Figure 4**). These results revealed that the mean uniformity coefficient (D_{60}/D_{10}) was the same at the eastern (T1) and western (T10) boundaries of the study site. In addition, most transects' uniformity coefficients (CU) remained between 1.65 and 1.72, while T3's and T4's uniformity coefficients were calculated to be 1.95 and 1.87 (**Figure 4**). This spike was due to T3-a's and T4-a's dramatic improvement in sorting, with CU values of 2.57 and 2.5. Despite certain improvement spikes in sorting

https://doi.org/10.59720/24-146

Figure 1: Location of Jones Beach, New York, and maps of sampling site distribution. a) Map specifying the location of Jones Beach relative to New York. **b)** Map of Jones Beach State Park outlining the distribution of the ten sampling transects utilized for this study at Jones Beach. **c)** Map displaying the a, b, and c-sites for T3, T4, and T5. Each transect's a-site is located in the low-tide zone, b-site in the middle-tide zone, and c-site in the high-tide zone. All images were adapted from Google Earth.

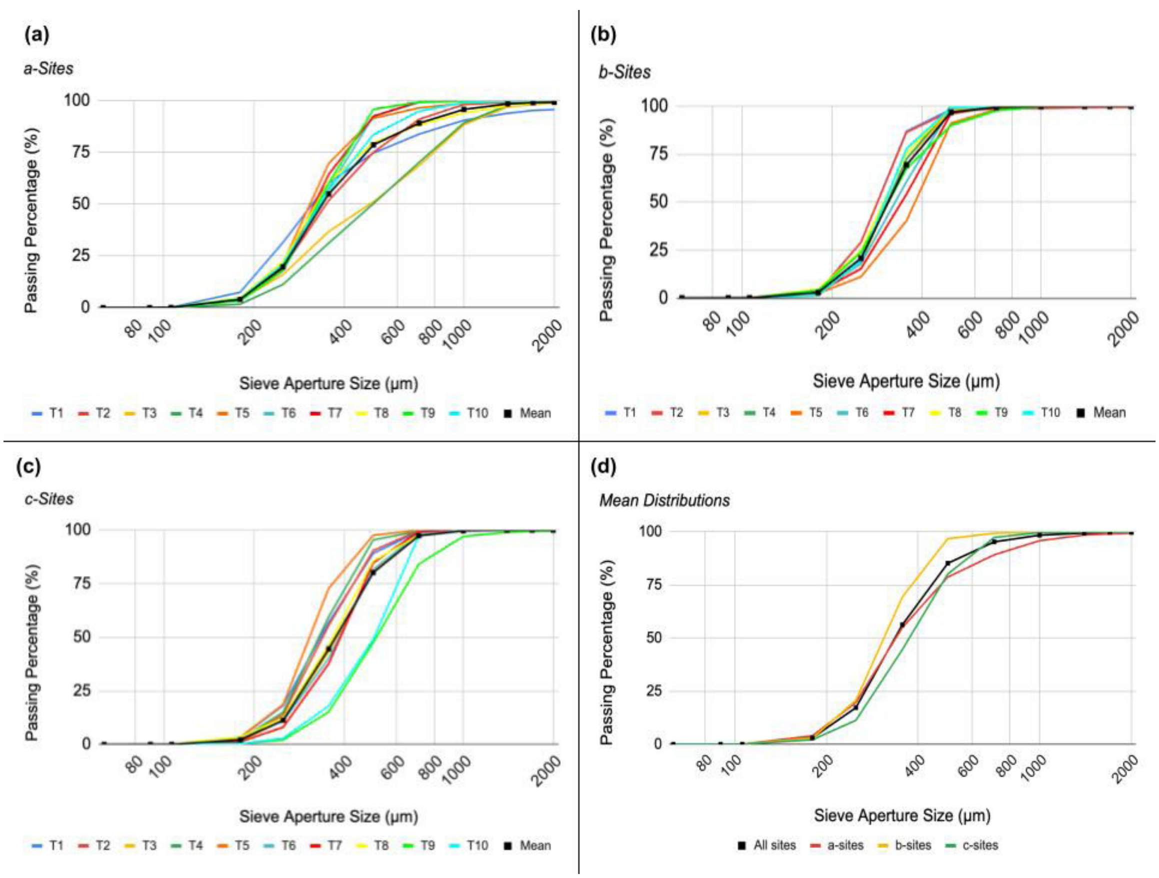

Figure 2: Cumulative passing percentages for sieve apertures increasing from 63 µm to 2 mm. Passing percentage values found between the 2 mm to the 63 µm sieve aperture for all sites compared to the mean distribution in their intertidal zone and the mean distributions for the **a)** low, **b)** middle, and **c)** high tide zone compared to the d) mean distribution for the entire study site. After a sample was sieved, the percent by weight of the sample that had passed through each sieve aperture was calculated and recorded.

https://doi.org/10.59720/24-146

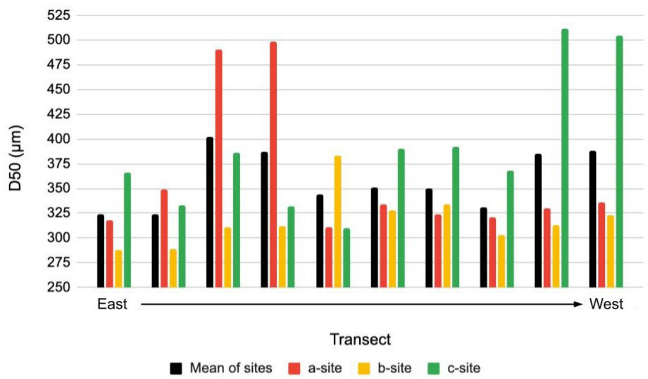

Figure 3: D_{50s} of each sampling site. The D_{50} calculated for each sample. a-sites were located in the study site's low-tide zone. b-sites were located in the study site's middle-tide zone. c-sites were located in the study site's high-tide zone. Cumulative passing percentage results were used to estimate the sieve aperture size at which cumulative passing percentage equaled fifty percent for each sample. Analysis of Variance (ANOVA) testing showed a significant difference ($p < 0.05$), with $F = 3.666$, and a critical F-value of 3.3541 at $\alpha = 0.05$. The mean D_{50} values of the a, b, and c-sites are significantly different from one another.

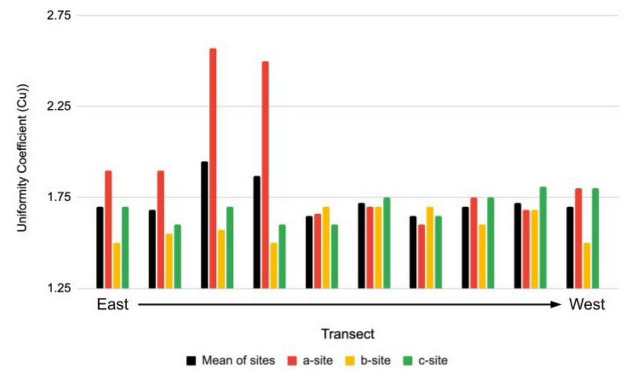

Figure 4: Uniformity coefficients (CU) of each sampling site. Uniformity coefficients (D_{60}/D_{10}) calculated for each sample. Cumulative passing percentage results were used to estimate each sample's D_{60} and D_{10}, whose quotient was calculated for each sample. Analysis of Variance (ANOVA) testing showed a significant difference ($p = 0.01$), with $F = 5.482$ and a critical F-value of 3.3541 at $\alpha = 0.05$. The mean CUs of the a, b, and c-sites are significantly different from one another.

at a few sites, the low tide zone's (a sites) sorting became slightly poorer (CU difference = -0.1), the high tide zone's (c sites) sorting slightly improved (CU difference = 0.1), and the middle tide zone's sorting was constant from T1 to T10, causing the site's average sorting constant to be equal at the eastern and western boundary of the study site (**Figure 4**).

At most transects, the sieve analysis results revealed that one of three intertidal regions had a coarser distribution, or larger D_{50}, than the average in that region across the site (**Figure 5**). Conversely, the other two intertidal areas at the same transect had finer distributions, or smaller D_{50s}, than their respective averages along the site (**Figure 5**). We designed passing percentage plots, which demonstrated that while the eastern region of the study site (T2 to T4) contained coarser than average a-sites (low tide zone) compared to the rest of the low tide zone, its b and c-sites were finer than the average of their respective intertidal sectors. Additionally, the middle region (T5, T6, and T7) experienced the same trend at its b-sites (middle tide zone), with its a and c-sites having been finer than their average intertidal-region distributions, and the western region (T9 and T10) displayed the trend at its c-sites (high tide zone), with its a and b-sites having been finer than their average intertidal-region distributions (**Figure 5**). Moreover, this coarseness trend appeared to be transferred from the low-tide zone of the study site's eastern region (T2 to T4) to the middle-tide region of T5 to T7 and then to the high-tide zone of T9 and T10, creating a diagonal-like trend in coarseness.

We observed a similar trend by estimating the D_{50} of every site: the sites that contained the coarser-than-average distributions also contained D_{50} values that were notably greater than the other sites in their respective intertidal zones. Furthermore, the estimated D_{50} values for T2-a, T3-a, and T4-a were 349 µm, 490 µm, and 498 µm, compared to the low-tide zone's mean D_{50} of 361 µm. All other a-sites displayed D_{50} values finer than the low-tide zone's mean D_{50} of 361 µm. In addition, the estimated D_{50} values for T5-b, T6-b, and T7-b were 383 µm, 328 µm, and 344 µm, while the average D50 of the middle-tide zone was 318 µm. In the high-tide zone, the average D_{50} was 389 µm, which all high-tide sites' D_{50s} were finer than, except T9-c and T10-c. T9-c and T10-contained D_{50s} were estimated to be much coarser at 512 µm and 504 µm, which made the northwestern region of the study site a coarse outlier. It is important to note that T8 displayed roughly the respective average D_{50} value in its low, middle, and high tide zones, making it an outlier in the above-described diagonal-like trend.

We found by examining the wave climate data that NDBC station 44065 experienced significantly more east-approaching than west-approaching significant wave action. Furthermore, NDBC station 44065 recorded 103,112 east-approaching significant waves compared to 27,983 west-approaching ones (**Figure 6**).

DISCUSSION

Applying the assumption of the McLaren model that sediment becomes finer and better sorted in the direction of transport, we hypothesized that the sediment along the coastline of Fields 4 and 5, Jones Beach, becomes progressively finer and better sorted from east to west. The results of our sieve analysis revealed that one of three intertidal regions at most transects had a coarser distribution than the average D_{50} in that region across the site. However, our results also revealed that the other two intertidal regions at the same transect had finer distributions than their respective average D_{50s} along the site. Starting in the low-tide zone of T1 and ending in the high-tide zone of T10, these trends created a diagonal-like trend from east to west of coarser than average sites surrounded by finer than average sites.

We used sieve apertures of 2 mm, 1 mm, 500 µm, 250 µm, and 63 µm for the sieve analysis because of their distinctive phi (ϕ) values and because 2 mm–63 µm is the sediment diameter range classified as sand by the Udden-Wentworth scale (26). Phi (ϕ) scaling GSD plots can help ensure that an equal focus is maintained between the larger and smaller diameters, and (ϕ) = -log2*d* (where d is particle diameter) (27). We utilized the additional apertures (1.7 mm, 1.4 mm, 710 µm, 355 µm, 180 µm, 106 µm, and 90 µm) to increase accuracy.

https://doi.org/10.59720/24-146

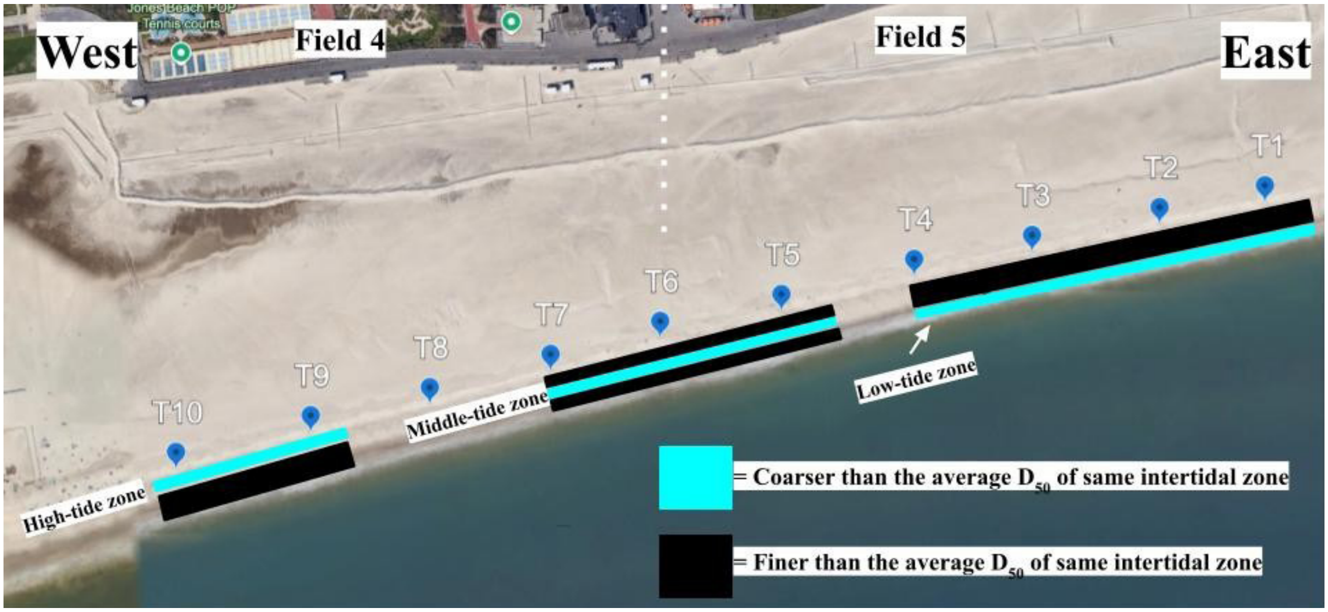

Figure 5: Observed sediment distribution trend at Jones Beach, New York. Diagram displaying the observed grain size distribution trend according to each site's variance from the mean D_{50} of the intertidal zone it is located in (adapted from Google Earth). Light blue lines represent where the study sites' D_{50s} were found to be coarser than the average D_{50} of their same intertidal zone (i.e., T10-c and T9-c have coarser D_{50s} than the average D_{50} for all c-sites). Black lines represent where the study sites' D_{50s} were found to be finer than the average D_{50} of their same intertidal zone.

Because the a-sites of T2, T3, and T4 were coarser than average while their middle and high-tide zones were finer than average, we hypothesized that there is a source of coarse sediment located east or southeast of the eastern boundary (T1) of Field 5. Additionally, although the findings suggest that incorporating apertures larger than 2 mm during sieve analysis for the study site is unnecessary because nearly 100% passing percentages were found at 2 mm at every site, future studies at different sites should prioritize the inclusion of apertures above this diameter to improve the accuracy of their sieve analysis results. Future studies should also prioritize the use of a laser grain-size analyzer over manual sieve analysis, which was not available for this study, thus limiting the accuracy of its results.

When used to interpret Fields 4 and 5's adjacent wave climate, NDBC station 44065 recorded significantly more east-approaching waves during the collection interval than west-approaching waves. These findings verify previous research stating that Jones Beach experiences oblique wave action predominantly in the east-to-west direction (24). However, the distance of NDBC station 44065 from Jones Beach–about 29 miles–limited the accuracy of applying the station's data to the wave climate adjacent to Jones Beach. Future experiments should prioritize the collection and use of directional wave climate data recorded closer to the study site to produce more accurate results that improve the understanding of the east-to-west mechanism of longshore drift at Jones Beach (24).

Analyzing the sieve analysis results in the context of the directional wave climate findings is essential for understanding sediment transport at the study site, as longshore currents are the primary cause of longshore sediment transport in the intertidal zone (28). Furthermore, because the site experiences predominantly east-approaching significant wave action, the sieve analysis results support the possibility that the coarse sediment introduced to the low-tide zone from T2 to T4 is gradually transported landward and west by the oblique-flowing, east-approaching waves.

We hypothesize that this trend in our findings forms because crashing (swash) waves initially transport immense amounts of the coarser grain in their flow direction but lose their redistribution force as they stretch landward and begin to recede. Thus, this difference in distribution force between swash and receding (backwash) would cause the coarser grain to be gradually transported more landward and west, resulting in the diagonal pattern of T2-a through T4-a (low tide), T5-b through T7-b (middle tide), and T9-c and T10-c (high tide) being the only coarser-than-average sites along their cross-shores (**Figure 2**). Future studies should further investigate this hypothesis by utilizing more transects over a larger study area that extends east and west of Fields 4 and 5. Furthermore, because directional sediment trends develop gradually along the shoreline, the availability of only sediment from Fields 4 and 5, Jones Beach, for this study limits the application of the theorized sediment transport model along other Jones Beach plots and coastal beaches.

The D_{50} and sorting findings from the sieve analysis agree with a previous study's interpretation that the application of the McLaren model is limited on beach faces (17). Specifically, mean D_{50} increased in the east-to-west direction of sediment transport at the study site, and while increasing in the high-tide zone, the mean uniformity coefficient at the site remained the same, indicating that sorting quality was constant. This contradicts the McLaren model prediction that sediment will be finer and better sorted in the transport direction (**Figure 7**). Moreover, our findings also differed greatly from previous research findings that sediment became finer and more poorly sorted in the transport direction, highlighting the differences

https://doi.org/10.59720/24-146

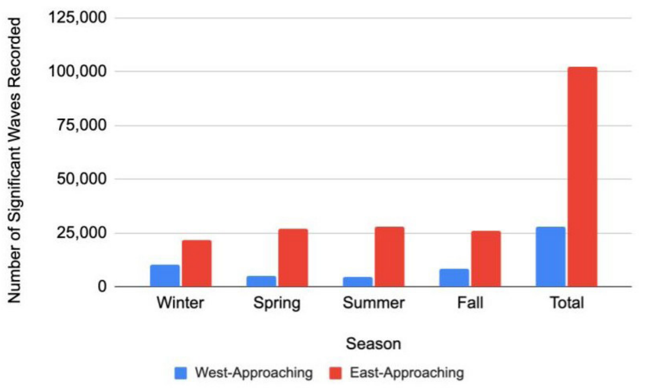

Figure 6: Cumulative number of significant waves recorded by National Data Buoy Center (NDBC) station 44065 during each season. Cumulative number of significant waves recorded by station 44065 during each season (29). Directional data for significant waves recorded by National Data Buoy Station 44065 from October 30th, 2008, to December 31, 2023, was collected and grouped into east-approaching and west-approaching waves, which were then grouped into the seasons when they were recorded.

in sediment transport systems from site to site (17). All in all, the uniqueness of this site's grain size trend and its sorting characteristics' contradiction to the literature display the need for further research on sediment transport to occur before generalizable sediment transport models can be applied to beach intertidal zones.

Modeling a coastline's GSD enhances the scientific understanding of how coastal sediments vary between sites, environments, and time periods. Understanding the site's sediment transport system is also imperative to the success of a beach nourishment project because the transport system helps to predict how nourishment sediment will redistribute over time (12). The sediment transport and GSD models created using the data collected at Jones Beach could assist in improving the overall understanding of sediment transport mechanisms and how oceanographic properties contribute to long-term shoreline evolution, potentially informing future beach enhancement projects at Jones Beach and coasts.

In summary, our hypothesis that the sediment along the coastline of Fields 4 and 5, Jones Beach, becomes progressively finer and better sorted from east to west was refuted by the findings: mean D_{50} increased in the direction of sediment transport, and mean sorting remained consistent at most transects. Overall, the findings and theorized sediment transport model at the study site are essential for potential future beach nourishment success at the study site. Our findings differed from several sediment transport trends reported in the literature (16-20). They also exhibited multiple discrepancies with the generalized trends proposed by the McLaren model for intertidal beach zones (16). U.S. coastlines continue to erode rapidly due to global warming and rising sea levels. In response, future research should investigate sediment transport trends on both high-energy and low-energy coasts, enabling the proper prediction and application of these trends to other coastlines. By accelerating beach nourishment while ensuring minimal long-term interference with on-site ecosystems, these evaluations can help sustainably reduce coastal erosion across the U.S.

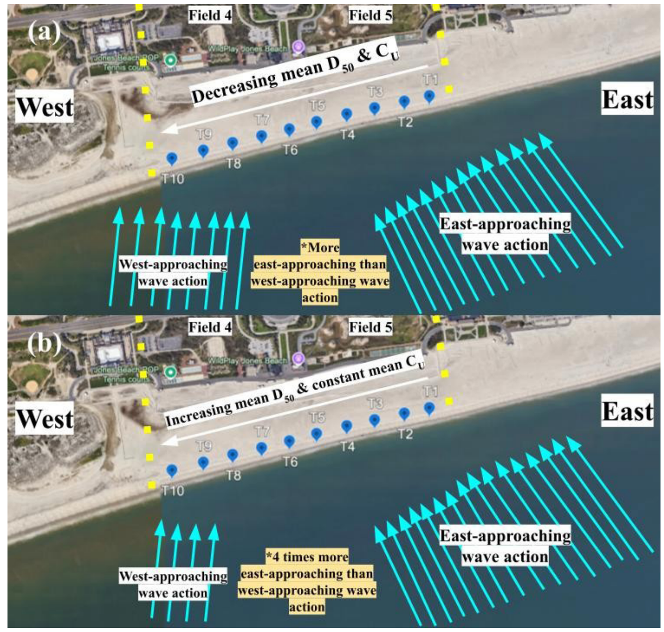

Figure 7: Hypothesized vs. observed sediment distribution patterns at Jones Beach, New York. a) Diagram displaying the hypothesized sediment distribution and directional wave approach trend at the study site at Jones Beach. **b)** Diagram displaying the observed sediment distribution and directional wave approach trend at the study site at Jones Beach. All pictures were adapted from Google Earth.

MATERIALS AND METHODS

Sample collection

We conducted a physical survey of the sediment in the intertidal zone of Fields 4 and 5, Jones Beach, New York. We virtually mapped 10 evenly spaced transects using the web-based version of Google Earth (accessed Jan. 2024) along the shore of Fields 4 and 5, Jones Beach, and designated cross-shore sites labeled a, b, and c on each transect in the respective low, middle, and high-tide zones, creating 30 sampling sites (**Figure 1**).

Beginning at peak low tide, we collected 50-gram surface-sediment samples from each sampling site from 0-1 cm deep using a handheld shovel and removed any seaweed, trash, and debris. We collected samples from the low-tide (a) sites first to ensure consistency and that the rising tide did not submerge them. We collected samples in NASCO Whirl-Pak® 4-1/2 X 9 in. 18 Oz. Polyethylene Write-On Bags because of their heat resistance (max. 82°C) and weight capacity.

Analysis preparation

We created two sieve stacks using six three-inch diameter sieves with a receiving pan on the bottom. The first sieve stack's apertures were 2 mm, 1.7 mm, 1.4 mm, 1 mm, 710μm, and 500 μm. The second sieve stack's apertures were 355 μm, 250 μm, 180 μm, 106 μm, 90 μm, and 63 μm. Before we constructed the sieve stacks, we used a digital balance to measure each empty sieve's weight to two decimal places and recorded these values. We dried the samples in their open sampling bags in an oven at 80°C until they were completely dry. After drying, we performed sieve analysis, during which we individually transferred samples into the first sieve stack, covering the stack with a sieve cover before agitating the stack for five minutes. After five minutes, we transferred the sample's remnants in the receiving pan into the second sieve stack and followed the same sieving process that we performed using the first stack. After the five-minute agitation period (a total of ten active sieving minutes) concluded, we disassembled the sieve stacks and weighed each full sieve and the second stack's receiving pan to two decimal places, i.e., determining the weight of each 50-gram sample that remained in each sieve after we completed the sieving procedures. We recorded each sieve's weight and calculated the difference between the sieve's full weight and empty weight. We used a Gilson Fine Sieve Cleaning Brush to thoroughly clean each sieve before sieving another sample. We repeated his process for each of the thirty samples. After completing the sieving and weight-difference recording procedures, we determined each sample's cumulative passing percentage values for each sieve aperture size by calculating the percentage of each sample, by weight, that passed through each aperture. We also calculated each sample's D_{50} and uniformity coefficient (CU). Using a TI-Nspire CX II CAS calculator, we then conducted a one-way Analysis of Variance (ANOVA) test on the calculated D50 values to compare the mean D50 value of each intertidal zone to one another. We then conducted the same statistical test on the calculated CU values.

We retrieved wave direction data from October 30th, 2008 (date of station deployment) to December 31st, 2023, from the National Data Buoy Center's (NDBC) station 44065, which is located about 29 miles southwest of the coast of Fields 4 and 5 and is the nearest station to the study site (29). We filtered and removed data denoted as suspect or missing by NDBC from the retrieved data (29). We utilized data from station 44065's initial deployment date until data collection occurred because distinct grain size trends develop slowly over time, making it beneficial to use the most directional data available. We filtered the remaining data based on their approaching direction, labeling 0.01 to 179.99 degrees as east-approaching and 180.01 to 359.99 as west-approaching. We then recorded the number of waves in each category. We applied these statistics to the Jones Beach site to examine Jones Beach's adjacent wave climate's influence on Fields 4 and 5's distributional grain size trends.

ACKNOWLEDGMENTS

We would like to thank Wantagh High School for funding the materials necessary to conduct the sieve analysis portion of this study.

Received: May 30, 2024
Accepted: September 23, 2024
Published: July 06, 2025

REFERENCES

1. "Coastal Erosion," *U.S. Climate Resilience Toolkit*. https://toolkit.climate.gov/topics/coastal-flood-risk/coastal-erosion. Accessed 10 Dec. 2023.
2. Saengsupavanich, C. "Elevated Water Level from Wind along the Gulf of Thailand." *Thalassas*, vol. 33, no. 4, 20 July 2017, pp. 179-185. https://doi.org/10.1007/s41208-017-0035-0.
3. "How Beach Nourishment Works." *US Army Corps of Engineers' Philadelphia District*. www.nan.usace.army.mil/Portals/37/docs/civilworks/SandyFiles/HowBeachNourishmentWorks.pdf. Accessed 16 Dec. 2023.
4. Matthews, D. H., and Wynes, S. "Current global efforts are insufficient to limit warming to 1.5°C." *Science*, vol. 376, no. 6600, 23 June 2022, pp. 1401-1409. https://doi.org/10.1126/science.abo3378.
5. "Climate Change: Global Sea Level" *NOAA*. www.climate.gov/news-features/understanding-climate/climate-change-global-sea-level. Accessed 11 December 2023.
6. "Climate Change Regulatory Actions and Initiatives." *Environmental Protection Agency (EPA)*, www.epa.gov/climate-change/climate-change-regulatory-actions-and-initiatives. Accessed 29 August 2024.
7. "Beach Nourishment." *Institute for Water Resources*, www.iwr.usace.army.mil/Missions/Coasts/Tales-of-the-Coast/Corps-and-the-Coast/Shore-Protection/Beach-Nourishment/. Accessed 30 May 2024.
8. "National Beach Nourishment Database." *ASBPA*. https://gim2.aptim.com/ASBPANationwideRenourishment. Accessed 16 January 2024.
9. Blott, S. J., and Pye, K. "Gradistat: A Grain Size Distribution and Statistics Package for The Analysis of Unconsolidated Sediments." *Earth Surface Processes and Landforms*, vol. 26, no. 11, 28 Sept. 2001, pp. 1237-1248. https://doi.org/10.1002/esp.261.
10. "Beach and shoreface nourishment." *Climate-ADAPT*. https://climate-adapt.eea.europa.eu/en/metadata/adaptation-options/beach-and-shoreface-nourishment. Accessed 30 May 2024.
11. Stauble, D. K. "A review of the role of grain size in beach nourishment projects." *U.S. Army Engineer Research and Development Center*, 2005. https://hdl.handle.net/1969.3/28926.
12. Narra, P., et al. "Sediment grain size variation along a cross-shore profile – representative d50." *Journal of Coastal Conservation*, vol. 19, no. 3, 24 May 2015, pp. 307-320. https://doi.org/10.1007/s11852-015-0392-x.
13. Román-Sierra, J., et al. "Influence of sieving time on the efficiency and accuracy of grain-size analysis of beach and dune sands." *The Journal of the International Association of Sedimentology*, vol. 60, no. 6, 8 Feb. 2013, pp. 1484-1497. https://doi.org/10.1111/sed.12040.
14. Kalore, S. A., and Sivakumar Babu, G. L. "Significance of Cu and Cc in Evaluating Internal Stability with Application to Design of Subbase Gradation in Pavements." *Transportation Geotechnics*, vol. 40, no. 3, May 2023. https://doi.org/10.1016/j.trgeo.2023.100972.
15. "Environmental Atlas of Lake Pontchartrain." *USGS*. https://pubs.usgs.gov/of/2002/of02-206/phy-environment/n-wave-climate.html. Accessed 11 August 2024.
16. McLaren, P. "An Interpretation of Trends in Grain Size Measures." *Journal of Sedimentary Research*, vol. 51, no. 2, 1 June 1981, pp. 611-624. https://doi.org/10.1306/212F7CF2-2B24-11D7-8648000102C1865D.
17. Masselink, G. "Longshore variation of grain size distribution along the coast of the Rhone Delta, Southern France: A test of the 'McLaren Model.'" *Journal of Coastal Research*, vol. 8, no. 2, Jan. 1992, pp. 286-291. https://jstor.org/stable/4297974.

https://doi.org/10.59720/24-146

18. Wu, J., and Shen, H. "Estuarine bottom sediment transport based on the 'McLaren Model': a case study of Huang Maohai Estuary, South China." *Estuarine Coastal and Shelf Science*, vol. 49, no. 2, Aug. 1999, pp. 265-279. https://doi.org/10.1006/ecss.1999.0495.
19. Vanwesenbeeck, V., and Lanckneus, J. "Residual sediment transport paths on a tidal sand bank: a comparison between the modified McLaren model and bedform analysis." *Journal of Sedimentary Research*, vol. 70, no. 2, May 2000, pp. 470–477. https://doi.org/10.1306/2dc40920-0e47-11d7-8643000102c1865d.
20. Lanckneus, J., et al. "The use of the McLaren model for the determination of residual transport directions on the Gootebank, Southern North Sea." *Progress in Belgian oceanographic research*, edited by J.C. Nihoul, pp. 75–94, Royal Academy of Belgium, 1993.
21. Gao, S., and Collins, M. "A critique of the "McLaren Method" for defining sediment transport paths." Journal of Sedimentary Research, vol. 61, no. 1, Jan. 1991, pp. 143-147. https://doi.org/10.1306/d42676a9-2b26-11d7-8648000102c1865d.
22. Mohd-Lokman, H., et al. "Deducing sediment transport direction and the relative importance of rivers on a tropical microtidal beach using the 'McLaren model.'" *Environmental Geology*, vol. 34, no. 23, May 1998, pp. 128–134. https://doi.org/10.1007/s002540050263.
23. Dipper, Frances. "Elements of Marine Ecology". *Elsevier Science*, 5th ed., 2022, pp. 1-35.
24. "What Makes Jones Beach a Classroom." *New York State Parks and Historic Sites.* https://nystateparks.blog/2022/03/02/what-makes-jones-beach-a-classroom/. Accessed 5 January 2024.
25. "Jones Beach State Park: Historic Structures & Cultural Landscape Report." *New York State Office of Parks, Recreation & Historic Preservation*, Accessed 18 March 2025.
26. Wentworth, C. K. "A Scale of Grade and Class Terms for Clastic Sediments." *The Journal of Geology*, vol. 30, no. 5, Jul. - Aug. 1922, pp. 377-392. https://doi.org/10.1086/622910.
27. Allaby, Michael. "Phi Scale." *A Dictionary of Earth Sciences*, edited by Michael Allaby, 3rd ed., Oxford University Press, 2008.
28. "Coastal Processes—Sediment Transport and Deposition." *National Park Service*. www.nps.gov/articles/coastal-processes-sediment-transport-and-deposition.htm. Accessed 29 May 2024.
29. "Historical NDBC Data." *National Data Buoy Center*, https://www.ndbc.noaa.gov/historical_data.shtml. Accessed 29 May 2024.